Molecular Plant Advance Access published March 21, 2014

Induced deactivation of genes encoding chlorophyll biosynthesis enzymes disentangles tetrapyrrole-mediated retrograde signalling

Hagen Schlicke, Annabel Salinas Hartwig, Vivien Firtzlaff, Andreas S. Richter, Christine Glässer[2], Klaus Maier[2], Iris Finkemeier[1], Bernhard Grimm*

Address: Institute of Biology/Plant Physiology, Humboldt University Berlin, Philippstr. 13, Building 12, D 10115 Berlin, Germany

[1] Max-Planck-Institute for Plant Breeding Research, Plant Proteomics and Mass Spectrometry Group, Carl-von-Linné Weg 10, 50829 Cologne, Germany

[2] Helmholtz Zentrum München, Deutsches Forschungszentrum für Gesundheit und Umwelt (GmbH), Ingolstädter Landstr. 1, 85764 Neuherberg

* To whom correspondence should be addressed: email: bernhard.grimm@rz.hu-berlin.de; Tel: +49 30 2093 6119

Running title: Plastid signalling in tetrapyrrole biosynthesis

Short Summary

Short-term inducible gene inactivation for the first three enzymatic steps in the Mg branch towards chlorophyll synthesis did not modify retrograde signalling-mediated nuclear gene expression. Long-term gene silencing of the same genes involved in tetrapyrrole biosynthesis causes either a pale-green or a necrotic leaf phenotype and feedback-regulated ALA synthesis or $^1O_2$-induced signalling affect nuclear gene expression.

Abstract

In photosynthetic organisms, tetrapyrrole-mediated retrograde signals are proposed to contribute to a balanced nuclear gene expression (NGE) in response to metabolic activity in chloroplasts. We followed an experimental short-term approach that allowed the assessment of modified NGE during the first hours of specifically modified enzymatic steps of the Mg branch of tetrapyrrole biosynthesis, when pleiotropic effects of other signals can be avoided. In response to 24 h-induced silencing of *CHLH*, *CHLM* and *CHL27* encoding the CHLH subunit of Mg chelatase, the Mg protoporphyrin methyltransferase and Mg protoporphyrin monomethylester cyclase, respectively, deactivated gene expression rapidly led to reduced activity of the corresponding enzymes and altered Mg porphyrin levels. But NGE was not substantially altered. When these three genes were continuously inactivated for up to 4 days, changes of transcript levels of nuclear genes were determined. *CHL27* silencing for more than 24 h results in necrotic leaf lesions and modulated transcript levels of oxidative stress-responsive and photosynthesis-associated nuclear genes (PhANGs). The prolonged deactivation of *CHLH* and *CHLM* results in slightly elevated transcript levels of PhANGs and tetrapyrrole-associated genes. These time-resolved studies indicate a complex scenario for the contribution of tetrapyrrole biosynthesis on NGE mediated by $^1O_2$-induced signalling and feedback-regulated ALA synthesis.

Keywords: plastid signal, transcription analysis, retrograde signal, tetrapyrrole metabolism, Mg protoporphyrin

Introduction

The genetic heterogeneity of photosynthetic organisms is explained by the origin of intracellular organelles, plastid and mitochondrion. Based on the endosymbiotic theory, engulfed microorganisms evolved to the specific organelles, which play crucial roles in energy conversion (Martin et al., 2002). The genetic and metabolic activities in these organelles require proteins, which are synthesized in a tightly coordinated expression of nuclear and plastid genes. The proteome of *Arabidopsis thaliana* plastids consists of approximately 3,000 proteins and its majority is encoded by nuclear genes. Only a few plastid-localized genes encode proteins which complete the complexes for photosynthesis, organellar gene expression and protein synthesis (Abdallah et al., 2000; Joyard et al., 2009; Leister, 2005). Functional organelles require mutual exchange of information between the nucleus and the organelles by anterograde and retrograde signalling, respectively. The nuclear gene expression (NGE) administers functionality of plastids and mitochondria by anterograde control. Thereby, the anterograde control coordinates not only the synthesis of nuclear-encoded proteins, but also their import into the organelles (Chi et al., 2013; Nott et al., 2006; Pesaresi et al., 2007; Pogson et al., 2008; Rodermel, 2001).

Retrograde signals emitted by components capable to sense and to communicate the developmental stage and the metabolic activities in chloroplasts and mitochondria (Rodermel, 2001). First experimental evidences for retrograde control of NGE indicated that photooxidative stress factors originating in the chloroplast transmit information to the nucleus to modulate NGE in response to the physiological state of plastids (Oelmuller and Mohr, 1986). Today it is known that multiple signals derived from various sources within the chloroplasts modulate NGE as a prerequisite for organelle development as well as for the adaption to several stresses and environmental changes. In the last decade, a multitude of reviews summarized the increasing number of published data, i.a. (Chi et al., 2013; Pogson et al., 2008; Woodson and Chory, 2012). The signals were grouped according to their emergence: (i) reactive oxygen species (ROS) and dedicated processes (Galvez-Valdivieso and Mullineaux, 2010; Kim and Apel, 2013), (ii) organellar redox state (Baier and Dietz, 2005; Brautigam et al., 2009), (iii) plastid protein synthesis (Gray et al., 2003; Pfannschmidt et al., 2009; Voigt et al., 2010), (iv) tetrapyrrole intermediates (Mochizuki et al., 2008; Moulin et al., 2008; Terry and Smith, 2013; von Gromoff et al., 2008; Woodson et al., 2011) and (v) metabolites, like 3-phosphoadenosine 5'-phosphate (PAP) (Estavillo et al., 2011),

methylerythritol cyclodiphosphate (MEcPP) (Xiao et al., 2012) and ß-cyclocitral ß-CC (Ramel et al., 2012).

The concept of plastid-derived retrograde signalling can be classified into two categories, the biogenic control and the operational control (Pogson et al., 2008). The biogenic control includes the bidirectional communication for the biogenesis of organelles at early developmental stages of seedlings. The operational control adjusts the organellar functions to the environmental changes by means of transducing signals from the plastids and modifying NGE. This concept implies that anterograde and retrograde signals are continuously required to enable optimal activity of plastids (and mitochondria) and to balance metabolic variations under normal and adverse environmental conditions. It is obvious that each plastid-derived signal is modulated by interaction with components of other signalling pathways (Chi et al., 2013; Estavillo et al., 2012). Hence, the optimized organellar function is a result of a combination and convergence of multiple signals.

Tetrapyrrole-mediated signalling has been proposed from the beginning of studies on retrograde signals (Kropat et al., 2000; Mochizuki et al., 2010; Nott et al., 2006; Susek et al., 1993; Terry and Smith, 2013). The tetrapyrrole biosynthetic pathway delivers essential, but also highly photoreactive end-products, which are capable of light absorption, but also prone to oxidants, such as molecular oxygen. Therefore, the metabolic pathway is subject of an intricate control system, including multiple feedback cues. Modulation of the rate limiting step of 5-aminolevulinic acid (ALA) synthesis, the initial steps of the chlorophyll-synthesizing Mg-branch and heme metabolism have been demonstrated to elicit a plastid-to-nucleus signalling for the coordination of NGE, in response to the physiological state of plastid-localized tetrapyrrole biosynthesis (Czarnecki et al., 2012; Larkin et al., 2003; Mochizuki et al., 2001; Strand et al., 2003; Woodson et al., 2011). In this context, the metabolite magnesium protoporphyrin (MgP) was suggested to act as a signal or secondary messenger molecule, once it is released from plastids. This hypothesis was tested by several research papers and questioned in reviews (Mochizuki et al., 2008, 2010; Moulin et al., 2008), because a correlation could not be demonstrated between steady-state levels of MgP and modulation of *LHCB* expression encoding light-harvesting chlorophyll-binding protein of photosystem II (LHCB) (Mochizuki et al., 2010), or any other photosynthesis-associated nuclear gene (PhANG) (Ruckle et al., 2007). Therefore, it remains open whether a potentially phototoxic compound could be a good candidate for a plastid-to-nucleus signalling molecule.

We aimed to specify and separate individual signals and asked whether tetrapyrrole biosynthesis releases plastid-derived signals that affect NGE. To assay tetrapyrrole-mediated retrograde signalling, it was necessary to induce modulation in metabolic activities of the pathway without a significant effect of physiological downstream processes. Thus, for the elucidation of a specific and unique tetrapyrrole signal for adjusting NGE, pleiotropic effects were avoided by ensuring intact and entire functional chloroplasts. This concept excludes the use of constitutive mutants, which are affected by mutation from the early embryogenesis, as well as the application of herbicides during germination as manipulators of plastid function, such as norflurazon. Instead, an inducible conditional gene deactivation of green adult plants was used to demonstrate an operational signalling from chloroplasts.

In this report, we focus on the assessment of potential retrograde signals derived from the tetrapyrrole biosynthesis pathway, particularly on magnesium porphyrins. Chemically induced short-term inactivation of genes involved in three successive enzymatic steps of chlorophyll biosynthesis, i.e. the insertion of Mg^{2+} into protoporphyrin (PIX) catalyzed by Mg chelatase, methyl esterification of MgP by MgP methyltransferase (CHLM), and the subsequent formation of an isocyclic ring from the 13-methyl propionate of magnesium protoporphyrin monomethylester (MgPME) by MgPME oxidative cyclase, were used to evaluate changes in NGE. Prior to the global transcript analyses of wild type and short-term modulated transgenic plants we confirmed that only the targeted enzymatic step of each transgenic line used in the studies was inactivated. In a proof of concept, we aimed to analyze to which extent initial modulations of tetrapyrrole biosynthesis releases signals for modulation of the transcriptome in green *Arabidopsis* seedlings.

Results

Short-term gene silencing causes rapid reduction of transcript levels and altered enzyme activities within 24 h

Transgenic *Arabidopsis* lines were generated carrying inducible RNAi transgene constructs for deactivation of the *CHLH* gene encoding the CHLH subunit of Mg chelatase, the *CHLM* gene encoding MgP methyltransferase, and the *CHL27* gene encoding the CHL27 subunit of MgPME cyclase. A single representative line was selected from the three sets of transgenic lines carrying the inducible gene inactivation construct for the respective target gene. This line is characterized by rapid gene deactivation following dexamethasone induction. The inducible gene deactivation was functional in the offspring of multiple generations within three years of the research period. The inactivation of each enzymatic step was compared to dexamethasone-treated wild type. Gene deactivation in 10-day-old seedlings reduced the mRNA content of *CHLH*, *CHLM*, and *CHL27* by more than 90% within 24 h after RNAi induction (Fig. 1A). Following the described short-term silencing, the seedlings did not display macroscopic phenotypes when compared to wild type (Fig. 1B).

Since the investigated RNAi lines phenotypically resembled wild-type seedlings 24 h after induced RNAi silencing, we first investigated changes in the metabolic pathway of chlorophyll biosynthesis. Decreased *CHLH*, *CHLM* and *CHL27* transcript levels resulted in a substantial reduction of activity of Mg chelatase, MgP methyltransferase or MgPME cyclase, respectively, in comparison to dexamethasone-treated wild-type seedlings (Fig. 1C-E). Because the short-term gene deactivation substantially lowered the activity of the targeted enzymes, the steady-state levels of tetrapyrrole intermediates were examined in seedlings after 24 h of induced RNAi silencing.

Although Mg chelatase activity decreased (Fig. 1C), it is remarkable that PIX, the substrate of Mg chelatase, did not accumulate in CHLH RNAi seedlings (Fig. 2A) in comparison to wild type, but magnesium porphyrins were not detectable (Fig. 2B/C). Lowered cyclase activity in CHL27 RNAi plants (Fig. 1E) resulted in a massive accumulation of MgPME (Fig. 2C), which is the substrate of the MgPME cyclase. Increased MgP steady-state levels (Fig. 2B) were also determined and most likely resulted from the tailback of porphyrin intermediates. Despite the reduced MgP methyltransferase activity (Fig. 1D), the CHLM RNAi line showed only a slight increase of porphyrin steady-state levels (Fig. 2A-C) 24 h after induced RNAi gene silencing. The reduced enzyme activities and altered Mg

porphyrin steady-state levels in all three RNAi lines, did not cause any changes in the chlorophyll contents compared to wild-type seedlings after 24-h-perturbation of the metabolic pathway (Fig. 2D). Interestingly, the ALA synthesis capacity was reduced in seedlings of the CHLH RNAi and CHLM RNAi lines (Fig. 2E). This observation agrees with the results previously obtained from *CHLH* and *CHLM* antisense tobacco lines (Alawady and Grimm, 2005; Papenbrock et al., 2000). The decreased ALA synthezising capacity after 24 h of RNAi silencing is proposed to be a consequence of the regulatory feedback, after deactivation of enzymes in the Mg branch (Cornah et al., 2003; Czarnecki and Grimm, 2012). The moderate increase of ALA synthesis capacity in the CHL27 RNAi line (Fig. 2E) resembles the elevated ALA synthesis observed in *LCAA* antisense tobacco lines, which showed reduced expression of this additional subunit of MgPME cyclase (Albus et al., 2012).

Modified porphyrin levels do not affect the expression of PhANGs and tetrapyrrole-associated genes

Although the short-term metabolic inactivation of gene expression caused reduced enzyme activities and modified Mg porphyrin levels, no macroscopic changes were detectable in the plants, including no changes in chlorophyll content (Fig. 2D). A transcriptome analysis of the three RNAi lines was performed 24 h after induction of RNAi gene silencing to investigate the effect of altered porphyrin steady-state levels on NGE. Ten-day-old seedlings were harvested from two different cultivations. The transcript profiling revealed 206, 188 and 206 differentially expressed genes in seedlings of the CHLH RNAi, CHLM RNAi and CHL27 RNAi line, respectively (Supplemental Table 1), with transcript levels deviating at least 2-fold compared to dexamethasone-treated wild type. Among the genes with altered transcript levels (Supplemental Table 1) no PhANGs, tetrapyrrole synthesis-associated genes or genes encoding components associated with any obvious chloroplast function were found. It is also important to emphasize that ROS marker genes proposed in (Galvez-Valdivieso and Mullineaux, 2010) are not distinctively up-regulated. Changes in expression of these genes have been previously associated with deregulation of tetrapyrrole biosynthesis and increasing photosensitization by accumulating porphyrins (Apel and Hirt, 2004; Kim et al., 2008).

Transcriptome analysis reveals a set of commonly deregulated genes as a side effect of the vector system

The evaluation of microarray data shows a group of 133 commonly deregulated genes after 24-h-deactivation of *CHLH*, *CHLM* and *CHL27* (Supplemental Table 2). However, an additional transcriptome analysis of a control RNAi line containing a pOpOff2(km):LUC gene construct that deactivates the *LUC* gene encoding firefly luciferase (Huang et al., 2011) was performed to prove whether the deregulation of NGE in the three lines is exclusively the result of disrupted tetrapyrrole biosynthesis (Fig. 3). This analysis presented in the Venn diagram revealed that 99 of the 133 genes were consistently either up- or down-regulated in the LUC RNAi line (Fig. 3A, Supplemental Table 2), indicating an integrative source of signals which leads to an altered NGE. Modified transcript levels of several genes analyzed in the microarray, were confirmed by quantitative reverse transcriptase polymerase chain reaction (qRT-PCR) (Supplemental Table 3). This indicates the quality and robustness of the transcriptomic data obtained by microarray analysis. Moreover comparative qRT-PCR analysis of dexamethasone-treated RNAi line and untreated-RNAi line revealed that the constitutive expression of the chimeric transcription factor encoded on the pOpOff2 vector did not yield altered mRNA amounts of investigated genes (data not shown). Thus, the analysis disclosed an unspecific effect on NGE triggered by the RNAi system possibly due to overexpression of small interference RNA (siRNA). The option that the chimeric transcription factor promotes also the expression of *Arabidopsis* endogenes after dexamethasone treatment needs to be further investigated.

The genes which were deregulated in at least one of the three RNAi lines and additionally in the LUC RNAi line show a similar deregulation (data not shown, Fig. 3B). The clusters without intersections to the LUC RNAi line contain the genes which were potentially deregulated as a result of impaired tetrapyrrole biosynthesis (Fig. 3B, Supplemental Table 4). Cluster 1 (Supplemental Table 4) includes all 34 genes which were commonly deregulated in the three RNAi lines for tetrapyrrole enzymes. A high number of these genes is also deregulated in the LUC-RNAi line but are not conform to the significance criteria. Cluster 5-7 (Supplemental Table 4) contains commonly deregulated genes in two RNAi lines each, while cluster 2-4 comprises of genes deregulated exclusively in one of the three RNAi lines for chlorophyll synthesis. It is worth to mention that the CHLM RNAi and CHLH RNAi lines share more common deregulated genes than any other twin combination, while the most exclusively deregulated genes are found in the CHL27 RNAi line after 24 h of significant inactivation of the cyclase activity. When all genes are assigned to GO categories, no significant over-representation of genes for specific categories could be derived using the the ***G****ene* ***O****ntology en****RI****chment ana****L****ysis and visua****L****iz****A****tion tool* (Eden et al., 2009) and the

deregulated genes of the LUC RNAi line as background set. Only the 99 commonly deregulated genes show an enrichment of the GO category defense response.

Using the software genevestigator (Hruz et al., 2008) expression profiles of the all deregulated genes upon gene silencing of chlorophyll-synthesis genes (cluster 1-7) were selected from publicly available comparative transcriptomic analyses of retrograde signalling mutants (*gun1, gun5*) with and without norflurazon treatment in comparison to wild-type controls. These tables in Supplemental Figure 1 indicate the variation of expression of these genes and allow comparison and potential assignment of these genes to typical PhANGs, which are characterized by a commonly accepted modulated expression pattern in *gun* mutants compared to wild type under adverse conditions, like norflurazon treatment. Among the analyzed 131 genes only eight genes were found showing a derepression of expression in the *gun* mutants compared to wild type after norflurazon treatment (Supplemental Figure 1). Further *in silico* analysis could not reveal any direct functional correlation between these genes and plastid function.

In summary, by means of the transcriptome analysis we could not assign specific sets of deregulated genes or single genes to functions in the plastid-nucleus communication and we conclude that 24 h of *CHLH*, *CHLM* and *CHL27* silencing did not likely address genes with certain significance in retrograde signalling.

Four-day-deactivation of chlorophyll biosynthesis genes causes drastic phenotypical changes

In continuation, the questions emerged how the RNAi lines adapted to the long-term silencing of *CHLH, CHLM*, and *CHL27*, and how the long-lasting deactivation of these genes affects NGE. For a 4-day-RNAi inactivation, the seedlings were grown on MS medium to ensure a constant supply of dexamethasone. For better differentiation between 24-h and 96-h-induced RNAi silencing, we refer to short-term and long-term gene silencing. We harvested seedlings after 1, 2 and 4 days of induced gene silencing. The transcript levels of the target genes *CHLH*, *CHLM*, and *CHL27* remained low or decreased further (Fig. 6G-I), indicating a continuously specific inhibition of the respective enzymatic step during the experimental procedure. Due to the inhibition of Mg chelatase reaction in the CHLH RNAi line, the downstream intermediates, such as MgP, MgPME and Pchlide, showed decreasing steady-state levels during the induction period, whereas PIX content increased approximately 3-fold

after a 4-day-repression of the *CHLH* expression (Fig. 4A). PIX did not drastically accumulate in comparison to wild type and, hence, did not cause leaf necrosis, as it can be observed after inhibition by herbicides or declined content of protoporphyrinogen oxidase 1 and ferrochelatase 2, respectively (Lermontova and Grimm, 2006; Papenbrock and Grimm, 2001). However, as a consequence of a reduced chlorophyll biosynthesis after 4 days of *CHLH* silencing, the newly developed leaves showed reduced green pigmentation (Fig. 4D, Fig. 5A) and an elevated chlorophyll a/b ratio in comparison to wild-type and the other transgenic seedlings (Fig. 5B).

The reduced MgP methyltransferase activity did not result in strong changes of intermediate steady-state levels (Fig. 4B). It is important to note that not even MgP, the substrate of CHLM, accumulated as a result of *CHLM* silencing. The CHLM RNAi line grew phenotypically similar to wild type (Fig. 4D) within the 4 days of continuously induced *CHLM* deactivation. In contrast, the limited MgPME cyclase activity in dexamethasone-treated CHL27 RNAi seedlings resulted in a continuous increase of its substrate, MgPME (Fig. 4C) to phototoxic concentrations and also in the weaker accumulation of the upstream intermediate MgP. The relative values of PIX and Mg porphyrins during the 4-day-gene silencing are depicted in Supplemental Table 5. Hence, necrotic leaf lesions (Fig. 4D) and, consequently, reduced chlorophyll contents (Fig. 5A) emerged after 4 days of *CHL27* silencing.

The ALA synthesis rate declined in the CHLH RNAi line already after 24 h of *CHLH* deactivation, while the CHLM RNAi line displayed only a slight reduction in ALA synthesis capacity within the 4-day-period. The ALA synthesis of the CHL27 RNAi line dropped after 2 days of gene silencing, and correlates with a photooxidative inactivation of pigment synthesis and the formation of leaf necrosis (Fig. 5D). The heme content was measured during the induced long-term gene silencing and no change was observed in all plants at any time of analysis with the exception of a reduced level (70% relative to wild type) in the CHL27 RNAi line after 4 days (Fig. 5D).

PhANGs show altered expression in the RNAi lines during long-term gene silencing

To monitor the impact of cumulative defects in plastid functions on NGE resulting from impaired chlorophyll biosynthesis, we investigated the kinetics of transcript accumulation of selected PhANGs, ROS marker genes and tetrapyrrole biosynthesis-associated genes within a

4-day-period of induced *CHLH*, *CHLM*, and *CHL27* gene silencing in comparison to time point zero (t_0). Keeping in mind that the PhANG transcript levels did not significantly change in the first 24 h after induced RNAi gene silencing, a normal PhANG expression correlates with normal plastid integrity (Terry and Smith, 2013). But the long-term deactivation of genes associated with early enzymatic steps of chlorophyll biosynthesis led to a differentiated pattern of modified transcript levels of selected PhANG representatives. The mRNA contents of *RBCS*, *LHCB1.2*, and *PC* encoding the small subunit of ribulose-1,5-bisphosphate carboxylase, LHCB of photosystem II, and plastocyanin, respectively, were moderately elevated in the CHLH RNAi and CHLM RNAi lines over the 4-day-period (Fig. 6D/E), compared to the corresponding transcript levels in wild type, while the transcript pattern of these three genes differed in the CHL27 RNAi line (Fig. 6F). After 4 days of *CHL27* silencing, the mRNA levels of PhANGs were drastically decreased and correlated with the formation of necrotic leaf tissue triggered most likely by photooxidative damage of accumulating Mg porphyrins (Fig. 4C).

Within 4 days of gene deactivation, the transcript accumulation of genes involved in the tetrapyrrole biosynthesis varied among the three RNAi lines (Fig. 6G-L). *FERROCHELATASE 1* (*FC1*) was the strongest up-regulated gene after 2 days of *CHL27* deactivation and indicates oxidative stress (Fig. 6L), as it was previously reported (Nagai et al., 2007). The CHLH RNAi line showed slightly elevated transcript levels of *HEMA1* and *GUN4* (3.5 and 3.0-fold, respectively) after four days of *CHLH* deactivation (Fig. 6J) and the CHLM RNAi line a 4.8-fold increase of *CHLH* mRNA (Fig. 6H). In agreement with our findings, the *CHLH* mRNA was accumulating in a *chlm* knock-out mutant (Pontier et al., 2007). But in general, the regulation of the tetrapyrrole biosynthesis genes in the CHLH RNAi and CHLM RNAi line were barely altered more than 2-fold in comparison to wild type. In conclusion, the transcript levels of genes encoding enzymes of ALA synthesis and the Mg branch tend to elevate during *CHLH* and *CHLM* silencing, while they were down-regulated within 4 days of *CHL27* deactivation.

To determine the role of ROS in response to impaired chlorophyll biosynthesis, we analyzed transcripts of ROS marker genes, such as *BONZAI1-ASSOCIATED PROTEIN* (*BAP1*), a $^1O_2$-responsive gene (op den Camp et al., 2003), *ZAT12*, a H_2O_2-responsive gene (Rizhsky et al., 2004), *FSD1* encoding plastid-localized Fe-superoxide dismutase 1 (Pulido et al., 2010), and *GPX7* encoding the plastid-localized glutathione peroxidase 7 (Mullineaux et al., 2000). The transcript levels of *GPX7* and *BAP1* increased more than 2-fold in the CHLH

RNAi line after 2 and 4 days of *CHLH* silencing, (Fig. 6A). While the expression of the ROS marker genes remained stable in the CHLM RNA line, in the CHL27 RNAi line the transcripts of *BAP1* and *ZAT12* accumulated substantially to more than 10-fold and 100-fold, respectively, and also *GPX7* mRNA content, although to a lesser extent, was also elevated (Fig. 6C).

Discussion

The synthesis of tetrapyrroles in plants depends on a tight control that follows the developmental program and demands of various environmental conditions, and is coordinated with production of apoproteins as well as the subsequent assembly of tetrapyrroles and proteins. Coordination of these processes is also ensured by a constant plastid-derived operational control (Pogson et al., 2008). Among multiple plastid-localized metabolites and regulatory mechanisms, which have been reported to emit retrograde signals, Mg porphyrins were suggested to act as retrograde signals to thereby control NGE (Strand et al., 2003). However, despite the broad range of proposed retrograde signalling components, very little is known about the significance of each molecule operating as a signal in the proposed signalling pathways.

In an effort to expand our understanding of tetrapyrrole-mediated signalling, we have studied the immediate (short-term) impact of modified tetrapyrrole biosynthesis on NGE, while interference of other signals, such as ROS, photosynthetic redox control, and altered chlorophyll content can be neglected. In compliance with the concept of permanent operational control by retrograde signals (Estavillo et al., 2012; Pogson et al., 2008), impaired plastid functions are expected to specifically emit and modulate retrograde signals exerting changes in NGE. Thus, in respect to tetrapyrrole biosynthesis, a specific inactivation of single metabolic steps in the pathway should instantaneously release retrograde signal(s).

To eliminate pleiotropic side effects from other signalling pathways, the dexamethasone inducible pOpOff2 vector system (Moore et al., 2006; Wielopolska et al., 2005) was used to enable a short-term deactivation of the *CHLH*, *CHLM*, and *CHL27* expression. We showed that a 24-h-induced gene silencing evidently promoted a substantial reduction of activities of Mg chelatase, MgP methyltransferase, and MgPME cyclase, respectively (Fig. 1C-E). Misbalanced steady-state levels of Mg porphyrins were observed (Fig. 2B-C), but no detectable effects on chlorophyll content were determined (Fig. 2D).

Deduced from seedling phenotype and chlorophyll content it is likely that during the early phase of RNAi gene silencing, photosynthesis and other physiological processes in the plastids were fully functional in the developed leaf cells.

Using a comparative microarray approach, we showed that the short-term gene silencing of *CHLH*, *CHLM*, and *CHL27* leads to an up- or down-regulation of 206, 188 and 206 genes, respectively. In this context it is important to note that most of these transcripts are solely regulated in response to the inducible RNAi vector system as it was shown by using the LUC RNAi control line (Fig. 3). It is known that the used RNAi system did not affect a broad range of physiological and morphological parameters (Huang et al., 2011). Nevertheless, further investigations could find out, whether either the over-expression of siRNA due to the induction of the inducible RNAi vector system or a direct modification of *Arabidopsis* gene expression caused by the dexamethasone-activated transcription factor itself are responsible for the observed changes of NGE.

The results of the transcriptome analysis obtained after short-term modified metabolic activity of the early steps in the Mg branch of tetrapyrrole biosynthesis, contradict an instantaneous modulation of NGE. Among the few genes, which are deregulated either commonly among the induced RNAi lines or exclusively in one of the transgenic lines, no gene was found which encodes a protein with a putative or established function in chloroplast or intracellular communication in response to plastid damages in wild type or in mutants of plastid retrograde signalling (Supplemental Table 1 and 4). The potential functions of these conspicuous genes of our transcriptome analysis could not be correlated to classes of genes required for responses to plastid damage, or modified metabolic activities in plastids. No PhANGs or genes encoding tetrapyrrole biosynthesis-associated proteins were identified among the deregulated genes after 24 h of induced RNAi inactivation (Supplemental Table 1).

Although changes of steady state levels of PIX and Mg porphyrins were observed within 24 h of gene silencing for enzymes of the Mg branch, changes of NGE in an immediate response of the accumulation of tetrapyrrole intermediates and their modified steady state levels could not be observed. These results are consistent with previous analyses, when no specific and unidirectional correlation between MgP accumulation and *LHCB1.2* expression was determined (Mochizuki et al., 2008; Moulin et al., 2008). Thus, independent short-term deactivation of the first three enzymes of the Mg branch seems not to be directly involved in retrograde signalling. Importantly, when metabolic changes in the tetrapyrrole biosynthesis pathway were observed (Fig. 2B/C) then regulatory consequences, e.g. reduced ALA

synthesis (Fig.2E), can already be measured. Due to high plasticity of chloroplasts, the short-term reduction of enzyme activities of the three first enzymatic steps of the Mg branch is apparently balanced in the entire pathway by posttranslational mechanisms. As long as deactivation of enzyme activities does not affect chlorophyll content or activate ROS signalling pathways caused by porphyrin accumulation, retrograde signalling in response to Mg porphyrin biosynthesis is not specifically modulated and, in consequence, distinct changes of transcript levels of nuclear genes are not induced.

These observations challenge the prevailing view that PIX and, in particular, Mg porphyrins are retrograde signals and tetrapyrrole metabolism at the stages of Mg porphyrin synthesis contributes to the plastid-derived signalling (Kindgren et al., 2012; McCormac and Terry, 2004; Strand et al., 2003). Many reports on plant tetrapyrrole-derived signalling are based on analysis of either constitutive mutants impaired in tetrapyrrole biosynthesis, which are or are not additionally treated with exogenous inhibitors, e.g. norflurazon. These studies were performed at early stages of seedling development and exemplified as biogenic control (Pogson et al., 2008), but were not possible to differentiate between induced tetrapyrrole- and ROS-dependent retrograde signalling. On the contrary, the inducible gene deactivation system expressed in green seedlings enabled us not only to explore the effects of potential emitters of retrograde signals exerting changes in NGE over the first hours and days following specific modulations of tetrapyrrole metabolism, but also provided sufficient amounts of plant tissue for genetic and biochemical analyses.

Long-term response to induced deactivation of enzymatic steps in chlorophyll biosynthesis

As significant transcriptional changes of nuclear genes for tetrapyrrole biosynthesis related proteins were not determined within the first 24 h of induced *CHLH*, *CHLM*, and *CHL27* silencing, we aimed to examine time-resolved changes in NGE in response to a deactivated Mg branch. After long-term RNAi-mediated gene silencing two different phenotypes could be differentiated among the transgenic lines in response to perturbed tetrapyrrole biosynthesis. In response to deactivated gene expression and reduced enzyme activity (Fig. 1A/C/D), the CHLH RNAi line and, to a lesser extent, the CHLM RNAi line represented pale green mutants (Fig. 4D) with reduced levels of metabolic products of the Mg branch (Fig. 4A/B). These lines are characterized by an attenuated metabolic flow of the pathway into the Mg

branch. In contrast, the CHL27 RNAi line accumulated phototoxic MgPME levels, which ultimately caused leaf necroses (Fig. 4C/D).

The steady-state levels of PIX and Mg porphyrins in response to inactivated *CHLH*, *CHLM* and *CHL27* expression reflect the modified control of the metabolic flow in the tetrapyrrole biosynthesis pathway, but do not necessarily correlate with potential retrograde signalling. A decelerated metabolic flow in response of *CHLH* and *CHLM* inactivation minimized the content of the products of these two enzymatic steps, while *CHL27* deactivation correlated instantaneously with the increasing contents of MgPME.

To date, retrograde signalling studies with mutant seedlings are aimed to elucidate potential roles and action mechanisms of the components of plastid-derived signalling, mainly during the acclimation to stress. The experimental strategy for the exploration of the mutants with defective genes encoding proteins of tetrapyrrole biosynthesis hampered the distinction between tetrapyrrole-mediated and other retrograde signalling pathways, including ROS- and redox-induced signaling, and led to pleiotropic phenotypes of bleaching or necroses of leaves and growth inhibition (Larkin et al., 2003; Meskauskiene et al., 2001; Mochizuki et al., 2001; Strand et al., 2003). We are aware that the effects of accumulating Mg porphyrins cannot ultimately be discussed without considering their photoreactive properties, and in consequence their cross-talk with other retrograde signalling pathways during light exposure (Nott et al., 2006; Pogson et al., 2008). Using the inducible RNAi system for three different enzymatic steps of the tetrapyrrole pathway, primary effects can be separated from secondary effects using time-resolved analyses as demonstrated here.

Considering the diverse phenotypes of the pale-green CHLH RNAi and CHLM RNAi lines versus the necrotic CHL27 RNAi line, the pattern of induced changes in NGE in each transgenic line correlated with either the distinct phenotype of reduced leaf pigmentation or necrotic leaf lesions. Each representative of the PhANGs as well as tetrapyrrole biosynthesis and ROS marker genes did not reveal similar kinetics during the 4-day-deactivation of either *CHLH*, *CHLM* or *CHL27*; instead, each analyzed gene indicated individual regulation of transcript accumulation (Fig. 6). Four-day-deactivation of *CHLH* and *CHLM* caused a slight accumulation of the *LHCB1.2*, *RBSC* and *PC* mRNA levels (Fig. 6D/E), while their transcript contents drastically decreased in the CHL27 RNAi line after 2 day of gene silencing compared to t_0 (Fig. 6F).

An induction of typical ROS marker genes was determined after 2 and 4 days following *CHL27* silencing (Fig. 6C) indicating an increasing oxidative stress rather than a tetrapyrrole biosynthesis-specific control. However, *GPX7* and *FSD1* normally responded to production of hydrogen peroxide (Mullineaux et al., 2000) and superoxide (Pulido et al., 2010) and were less induced than *ZAT12 and BAP1* in the CHL27 RNAi line. *BAP1* is known as singlet oxygen ($^1O_2$)-responsive gene (op den Camp et al. 2003). We suggest that the excessive MgPME accumulation in light-exposed seedlings (after 1d, Fig. 2C) generates $^1O_2$, which induces ROS-mediated retrograde signalling leading to induction of ROS marker genes (2d, Fig. 6C) and suppression of PhANGs and tetrapyrrole biosynthesis genes (Fig. 6F, I, L). These processes presumably resemble consequences of Pchlide accumulation in light-dark grown *flu* mutants (Meskauskiene et al., 2001) and it is hypothesized that the pattern of modified NGE of the long-term inactivated CHL27 RNA line is similar to $^1O_2$-induced *flu* transcriptome (op den Camp et al., 2003). In contrast to RNAi-mediated *CHL27* inactivation, none of the investigated ROS-responsive transcripts accumulated after *CHLH* and *CHLM* deactivation (Fig. 6A/B).

The Arabidopsis CHLH RNAi and CHLM RNAi lines resemble transgenic tobacco plants expressing either *CHLH* or *CHLM* antisense RNA (Alawady and Grimm, 2005; Papenbrock et al., 2000). In agreement with these reports, inactivation of the first two enzymes of the Mg branch results in suppression of ALA synthesis (Fig. 5D) and, consequently, lower PIX and Mg porphyrin contents. The altered transcript levels of PhANGs and genes of tetrapyrrole biosynthesis upon the long-term *CHLH* and *CHLM* deactivation is associated with reduced chlorophyll content, impaired photosynthesis, and/or reduced feed-controlled ALA biosynthesis. Future studies are necessary to verify the multiple retrograde signals which are derived from ALA synthesis, chlorophyll deficiency and diminished photosynthesis capacity and contribute to the control of NGE. In this context, two independent sets of *Arabidopsis* seedlings with reduced ALA synthesis contain an overlapping class of deregulated genes: the *gun4-1* knock-down mutant and seedlings upon inhibition of gabaculine (inhibitor of glutamate 1-semialdehyde aminotransferase, the second enzyme of ALA biosynthesis) (Czarnecki et al. 2012). It can be hypothesized that long-term inactivation of Mg chelatase and MgProto methyltransferase deregulates an overlapping set of genes similar to direct reduction of ALA synthesis

In contrast, short-term inactivated *CHL27* expression tends to stimulate ALA biosynthesis, as is was previously reported in response to reduced expression of the cyclase

subunit LCAA/YCF54 (Albus et al., 2012). But, after 2 days of induced gene deactivation, ALA biosynthesis is down-regulated. The induced ROS marker genes and the necrotic leaf spots are indicative for photooxidative stress after two days of *CHL27* deactivation (Fig. 6C). Experimental evidence for oxidative stress-inactivated ALA biosynthesis has been previously presented (Aarti et al., 2007).

The heme content in all three transgenic lines was not altered during the investigation period in comparison to wild type, although the metabolic flow in tetrapyrrole biosynthesis was substantially affected by deactivation of the enzymatic steps in chlorophyll biosynthesis. An inhibitory effect of heme on the ALA synthesis rate at the posttranslational level was proposed previously (Pontoppidan and Kannangara, 1994; Srivastava et al., 2005). Moreover, *Arabidopsis* ferrochelatase 1 overexpressor lines accumulate more PhANGs upon norflurazon inhibition than wild type and heme synthesis is proposed to be associated with upregulation of PhANGs (Woodson et al., 2011). Therefore, the existence of further regulatory mechanisms affecting the rate-limiting steps of ALA formation by the transcriptional and posttranslational control are likely and can be mediated by regulatory heme pools and chlorophyll availability.

In conclusion, NGE deregulation in response to deactivation of enzymatic steps of chlorophyll biosynthesis and changes in Mg porphyrin levels is only observed after more than 1 day of gene deactivation and follows different regulatory mechanisms, which are specific for the inactivated step. Changes in NGE by *CHLH* and *CHLM* deactivation correlate with reduced chlorophyll content and attenuated metabolic flow in the tetrapyrrole biosynthetic pathway. Long-term *CHL27* deactivation induces the expression of genes by a ROS-dependent signalling pathway, while PhANGs and genes of tetrapyrrole biosynthesis tend to be down-regulated. These changes correlate with transcriptional control of NGE in response to MgPME-induced $^1O_2$ formation (Laloi et al., 2007). It will be important in future to pay attention to the integration of different retrograde signalling pathways, which are triggered by metabolites and environmental signals in chloroplast and induce collectively NGE.

Experimental Procedures

Biological Material, Growth Conditions and Treatment

To generate dexamethasone-inducible RNAi pOpOff2 lines specific sequences of the corresponding coding regions (Supplemental Table 6) were cloned into pDONR221

(Invitrogen). The target fragments were subsequently recombined into the destination vector pOpOff2(hyg) (Wielopolska et al., 2005) using the GATEWAY™ system (Invitrogen). After *Agrobacterium* mediated transformation, seeds of the F1 generation of CHLH RNAi, CHLM RNAi and CHL27 RNAi lines were selected on MS plates containing hygromycin (35 µg/ml). The LUC RNAi line targets the firefly luciferase and was previously introduced including the description of potential secondary effects of the RNAi system used (Huang et al., 2011). The RNAi system includes i.a. a gene encoding a constitutively expressed chimeric transcription factor, which binds with dexamethasone to the pOp6 promoter for expression of RNAi cassette.

The *Arabidopsis* wild type (Col-0) and transgenic RNAi lines were grown on soil at 110 µmol photons m^{-2} s^{-1} under short day (10 h light) conditions, acclimated for at least three days in continuous light and sprayed with dexamethasone (20 µg/ml). The kinetic data are generated from 14-d-old seedlings grown on MS medium at 100 µmol photons m^{-2} s^{-1} continuous light, subsequently transferred to dexamethasone (20 µg/ml) containing MS plates.

Extraction and HPLC Analysis of Porphyrins and Pigments

Samples from wild-type and transgenic seedlings were frozen, homogenized with a ball-mill and freeze-dried. Powdered samples were suspended in ice-cold acetone/0.1 M NH_4OH (9/1, v/v), centrifuged and analyzed. Chlorophyll, heme and tetrapyrrole metabolites were analyzed according to (Kim et al., 2013) and PIX according to (Scharfenberg et al., 2013). MgP and MgPME were separated on a Poroshell 120 EC-C18 (Agilent) column (2.7 µm; 150 x 3.0 mm; 21°C) at a flow rate of 0.55 ml min^{-1} and isocratic eluted with 90 % of solvent A (90 % methanol; 10 % 1M ammonium acetate pH 7.0) and 10 % of solvent B (100 % ethyl acetate). Porphyrins were quantified at λ_{Ex} 420 nm and λ_{Em} 600 nm (peak width 2.31 Hz; PMT gain 17) using authentic standards.

ALA Synthesis Capacity

Arabidopsis seedlings were harvested after treatment with dexamethasone, incubated for 4 h in 40 mM levulinic acid and TRIS/HCL buffer (pH 7.2) and analyzed according to (Mauzerall and Granick, 1956) with modifications (Richter et al., 2013). Frozen samples were ground in a ball mill, resuspended in 20 mM potassium phosphate buffer (pH 6.8) and centrifuged. Four hundred µl of the supernatant was mixed with 100 µl ethyl acetoacetate, boiled for 10 min and

chilled to room temperature. After adding modified Ehrlich´s reagent, the absorption of the ALA pyrrole was measured at 553 nm. ALA quantification based on at least three biological replicates using a standard curve of ALA.

Transcript Analysis

Total RNA was extracted from *Arabidopsis* seedlings using TRIsure reagent (Bioline) and 2 µg RNA was used for DNase treatment and reverse transcription (Thermo Fisher Scientific) using oligo-dT_{18} following manufacturer´s protocol. The qRT-PCR was performed using Sensi-Mix (Bioline) and a BFX96 thermo cycler (Biorad) with the following program: 10 min at 95°C, 45 cycles of 15 sec at 95°C, 15 sec at 60°C and 15 sec at 72°C. Calculation of relative expression levels was performed according to (Livak and Schmittgen, 2001) using *AtACT2* (At3g18780) as reference genes. The Supplemental Table 7 shows the primer pairs used for transcript analysis.

Microarray Analysis, Data Normalization, Differential Expression and Heat Map

Microarray analysis was performed using the ATH1 *Arabidopsis* Gene Chip. The quality control of RNA and hybridization was performed at Nottingham *Arabidopsis* Stock Centre (UK). Analysis of differential expression was conducted using the LIMMA package (Smyth, 2004) and Bioconductor (Gentleman et al., 2004) in R. Affymetrix spots were translated to TAIR10 annotation using the cdf file provided by http://nmg-r.bioinformatics.nl/NuGO_R.html. Expression was calculated by applying the function just.rma with standard settings (robust multi-array average expression measure, RMA) (Irizarry et al., 2003) as background correction, quantile normalization) and differential expression calculation was subsequently carried out using an empirical Bayes linear modeling approach. The resulting p-values were corrected according to (Benjamini and Hochberg, 1995). Genes were considered to be significantly deregulated when their respective p-value was ≤ 0.05 and the fold change was 2 fold. All genes being differentially expressed were depicted in a heat map using function heatmap.2 implemented in the R stats package. The scaling was based on rows, thus left at default, while the colors were set to an interpolation of blue and yellow.

Chloroplast Isolation and Enzyme Activity Assays

Chloroplasts were extracted from three- to four-week-old seedlings grown on soil and treated with dexamethasone for 24 h. The plant material was homogenized in precooled extraction

buffer (0.8 M sorbitol, 40 mM Tricine-KOH; pH 8.0; 20 mM $NaHCO_3$, and 0.2 % bovine serum albumin (BSA), filtered through Miracloth (Merck Millipore), centrifuged at 500 g for 8 min, and the pellet was resuspended in extraction buffer without (BSA). The crude chloroplast extracts were used for enzyme activity measurements using the assay buffer (0.8 M sorbitol, 40 mM Tricine-KOH; pH 8.0; 20 mM $NaHCO_3$, 25 mM $MgCl_2$, 1 mM DTT, and 0.2 % BSA). The Mg chelatase activity was assayed with modifications as previously described (Peter and Grimm, 2009). The chloroplast extract was mixed with an equal volume of assay buffer and 16 mM ATP and 20 µM PIX, 800 rpm, 30 °C, in darkness. After centrifugation the MgP content was measured via HPLC analysis as described above. The protocol of the methyltransferase assay was adapted from (Richter et al., 2013), whereas the assay buffer is supplemented with 1 mM S-adenosyl-methionine and 40 µM MgP. For the cyclase assay, 10 mM NADPH and 12 µM MgPME were added. For enzyme assays, the catalytic product was quantified using tetrapyrrole standards (see above), except for the cyclase assay, when the rate of metabolized substrate was measured.

Supplementary Data

Supplementary Tables are available at Molecular Plant Online

Acknowledgments

We would like to thank Ian Moore (Oxford University, UK) for providing the pOpOff2(kan)::LUC control transgenic line. We thank Pawel Brzezowski and Boris Hedtke for critically reading the manuscript. This work was supported by grants of the Deutsche Forschungsgemeinschaft (FOR 804).

Figure Legends

Figure 1. Genetic and biochemical analysis of transgenic lines after 24 h gene silencing of *CHLH, CHLM* and *CHL27*, respectively.

(A) Transcript analysis of 10-day-old seedlings of the CHLH, CHLM and CHL27 RNAi lines growing on MS in continuous light 24 h after induced gene silencing. Transcript levels were calculated as relative expression ($2^{-\Delta\Delta CT}$) according to (Livak and Schmittgen, 2001) in comparison to dexamethasone-treated wild-type plants as control and *Actin2* as a reference

gene. The *CHLH*, *CHLM* and *CHL27* transcript contents were decreased in the corresponding RNAi lines to less than 10% of the wild type content. Data are given as means and SD of three biological replicates. (B) Phenotypes of 14-day-old *Arabidopsis* wild-type and RNAi lines. Seedlings grew in continuous light of 100 µmol photon m^{-2} s^{-1} treated for 24 h with dexamethasone. (C-E) Enzyme activity assays with crude *Arabidopsis* chloroplast extracts 24 h after induction of RNAi silencing for (C) Mg chelatase (MgCh), (D) MgP methyltransferase (MT) and (E) MgPME cyclase (Cyc) given as metabolic rate of the substrate. Data are given as means and SD of three biological replicates. All experiments were repeated at least two times.

Figure 2. Chlorophyll content and steady state levels of tetrapyrrole biosynthesis intermediates 24 h after *CHLH*, *CHLM* and *CHL27* gene silencing.

(A-C) Steady state levels of porphyrins 24 h after treatment with dexamethasone and induced RNAi gene silencing. A. protoporphyrin IX (PIX), B. magnesium protoporphyrin (MgP), C. MgP monomethylester (MgPME). (D) The chlorophyll content of seedlings of the three RNAi lines and wild type determined 24 h after induced gene silencing. (E) Analysis of the ALA synthesizing capacity in transgenic lines in comparison to wild type after 24 h of induced *CHLH*, *CHLM* and *CHL27* gene silencing. Plants were grown on soil for 14 days under 100 µmol photon m^{-2} s^{-1} light intensity.

Figure 3. Comparative microarray analysis of CHLH, CHLM, CHL27 and LUC RNAi lines 24 h after RNAi induction.

(A) Heat map analysis of commonly deregulated genes 24 h after induction of RNAi in the four RNAi lines. The LUC RNAi line contains a part of the firefly luciferase gene sequence which did not interfere with *Arabidopsis thaliana* transcripts after activation of the RNAi machinery. Genes showing a twofold increase or decrease of the fold change (FC) compared to wild type and a *P*-value of less than 0.05 in all four RNAi lines were depicted. Almost all these genes are uniformly deregulated. (B) The Venn diagram shows the central cluster of 99 commonly deregulated genes 24 h after dexamethasone activation of the RNAi mechanism. The intersections represent the number of mutually deregulated genes in the corresponding RNAi lines. The Supplemental Table 2 contains the lists of genes representing the intersections.

Figure 4. Kinetics on steady state levels of PIX and Mg porphyrins within a 4-day-silencing of genes encoding proteins of chlorophyll biosynthesis.

(A-C) Time course of porphyrin steady state levels 1, 2 and 4 days after induced RNAi gene silencing of *CHLH*, *CHLM* and *CHL27* compared to the time point t_0. PIX, protoporphyrin, MgP, magnesium protoporphyrin, MgPME, MgP monomethylester, and Pchlide, protochlorophyllide were analyzed. (D) Phenotypes of *Arabidopsis* wild-type and RNAi lines seedlings growing in continuous light of 100 µmol photon m^{-2} s^{-1} after a long-term dexamethasone-induced *CHLH*, *CHLM* or *CHL27* gene silencing.

Figure 5. Analysis of chlorophyll and heme content as well as ALA capacity in wild type and transgenic RNAi lines in the course of 4-day deactivation of early enzymatic steps in the Mg branch of tetrapyrrole biosynthesis.

(A) Relative chlorophyll content compared to time point t_0 for each line. The wild type chlorophyll content at time point t_0 is 12.2 nmol mg^{-1} dw. (B) The chlorophyll *a* /chlorophyll *b* ratio in wild type and the three RNAi lines. (C) Relative heme content in of transgenic lines compared to wild type for each time point. The wild type has a heme content of 1.2 pmol mg^{-1} dw at t_0. The heme content is not significantly altered in the RNAi lines within the 4 days of gene inactivation. (D) ALA synthesizing capacity of the three RNAi lines compared to wild type for each time point. The t_0 value of wild type corresponds to 0.36 nmol ALA mg^{-1} fw h^{-1}.

Figure 6. Analysis of the transcript levels of nuclear genes in the CHLH, CHLM and CHL27 RNAi lines during a time course of 4-day-induction of RNAi.

(A-C) Transcript analysis of ROS marker genes. *BAP1* a $^1O_2$-responsive gene and *ZAT12* a H_2O_2 responsive gene encoding bonzai1-associated protein 1 and zinc finger protein, respectively. *GPX7* and *FSD1* encode the plastid-localized glutathione peroxidase 7 and Fe-superoxide dismutase, respectively. (D-F) Transcript analysis of the representatives of PhANGs, *RBCS*, *LHCB1.2* and *PC* encoding ribulose 1,5-bisphosphate carboxylase small subunit, LHCB of photosystem II and plastocyanin, respectively.(G-I) Analysis of mRNA amounts of genes encoding enzymes of the Mg branch of tetrapyrrole biosynthesis. *CHLH* and *CHLD* encode the CHLH and CHLD subunit of Mg chelatase,. *CHLM* and *CHL27* encode MgP methyltransferase and the CHL27 subunit of MgPME cyclase, respectively. (J-L) Analysis of mRNA amounts of genes encoding target proteins of tetrapyrrole biosynthesis. *HEMA1*, *GUN4*, *PORB* and *FC1* encode the glutamyl-tRNA reductase 1, GUN4, a positive regulator of the Mg chelatase reaction, protochlorophyllide oxidoreductase B and ferrochelatase 1, respectively. Transcript levels were calculated as relative expression ($2^{-\Delta\Delta CT}$)

according to (Livak and Schmittgen, 2001) in comparison to t_0 and *Actin2* as a reference gene. Data are given as means and SD of three biological replicates summarized in the Supplemental Table 8. Plants were grown on MS for 14 days under continuous light (100 µmol photon m^{-2} s^{-1}).

References

Aarti, D., Tanaka, R., Ito, H., and Tanaka, A. (2007). High light inhibits chlorophyll biosynthesis at the level of 5-aminolevulinate synthesis during de-etiolation in cucumber (Cucumis sativus) cotyledons. Photochem Photobiol 83:171-176.

Abdallah, F., Salamini, F., and Leister, D. (2000). A prediction of the size and evolutionary origin of the proteome of chloroplasts of Arabidopsis. Trends Plant Sci 5:141-142.

Alawady, A.E., and Grimm, B. (2005). Tobacco Mg protoporphyrin IX methyltransferase is involved in inverse activation of Mg porphyrin and protoheme synthesis. Plant J 41:282-290.

Albus, C.A., Salinas, A., Czarnecki, O., Kahlau, S., Rothbart, M., Thiele, W., Lein, W., Bock, R., Grimm, B., and Schottler, M.A. (2012). LCAA, a novel factor required for magnesium protoporphyrin monomethylester cyclase accumulation and feedback control of aminolevulinic acid biosynthesis in tobacco. Plant Physiol 160:1923-1939.

Apel, K., and Hirt, H. (2004). Reactive oxygen species: metabolism, oxidative stress, and signal transduction. Annu Rev Plant Biol 55:373-399.

Baier, M., and Dietz, K.J. (2005). Chloroplasts as source and target of cellular redox regulation: a discussion on chloroplast redox signals in the context of plant physiology. J Exp Bot 56:1449-1462.

Benjamini, Y., and Hochberg, Y. (1995). Controlling the false discovery rate: a practical and powerful approach to multiple testing. Journal of the Royal Statistical Society Ser. B 289-300.

Brautigam, K., Dietzel, L., Kleine, T., Stroher, E., Wormuth, D., Dietz, K.J., Radke, D., Wirtz, M., Hell, R., Dormann, P., et al. (2009). Dynamic Plastid Redox Signals Integrate Gene Expression and Metabolism to Induce Distinct Metabolic States in Photosynthetic Acclimation in Arabidopsis. Plant Cell.

Chi, W., Sun, X., and Zhang, L. (2013). Intracellular signaling from plastid to nucleus. Annu Rev Plant Biol 64:559-582.

Cornah, J.E., Terry, M.J., and Smith, A.G. (2003). Green or red: what stops the traffic in the tetrapyrrole pathway? Trends Plant Sci 8:224-230.

Czarnecki, O., Glasser, C., Chen, J.G., Mayer, K.F., and Grimm, B. (2012). Evidence for a Contribution of ALA Synthesis to Plastid-To-Nucleus Signaling. Frontiers in plant science 3:236.

Czarnecki, O., and Grimm, B. (2012). Post-translational control of tetrapyrrole biosynthesis in plants, algae, and cyanobacteria. J Exp Bot 63:1675-1687.

Eden, E., Navon, R., Steinfeld, I., Lipson, D., and Yakhini, Z. (2009). GOrilla: a tool for discovery and visualization of enriched GO terms in ranked gene lists. BMC Bioinformatics 10:48.

Estavillo, G.M., Chan, K.X., Phua, S.Y., and Pogson, B.J. (2012). Reconsidering the nature and mode of action of metabolite retrograde signals from the chloroplast. Frontiers in plant science 3:300.

Estavillo, G.M., Crisp, P.A., Pornsiriwong, W., Wirtz, M., Collinge, D., Carrie, C., Giraud, E., Whelan, J., David, P., Javot, H., et al. (2011). Evidence for a SAL1-PAP chloroplast retrograde pathway that functions in drought and high light signaling in Arabidopsis. Plant Cell 23:3992-4012.

Galvez-Valdivieso, G., and Mullineaux, P.M. (2010). The role of reactive oxygen species in signalling from chloroplasts to the nucleus. Physiol Plant 138:430-439.

Gentleman, R.C., Carey, V.J., Bates, D.M., Bolstad, B., Dettling, M., Dudoit, S., Ellis, B., Gautier, L., Ge, Y., Gentry, J., et al. (2004). Bioconductor: open software development for computational biology and bioinformatics. Genome Biol 5:R80.

Gray, J.C., Sullivan, J.A., Wang, J.H., Jerome, C.A., and MacLean, D. (2003). Coordination of plastid and nuclear gene expression. Philos Trans R Soc Lond B Biol Sci 358:135-144; discussion 144-135.

Hruz, T., Laule, O., Szabo, G., Wessendorp, F., Bleuler, S., Oertle, L., Widmayer, P., Gruissem, W., and Zimmermann, P. (2008). Genevestigator v3: a reference expression database for the meta-analysis of transcriptomes. Advances in bioinformatics 2008:420747.

Huang, W., Ling, Q., Bedard, J., Lilley, K., and Jarvis, P. (2011). In vivo analyses of the roles of essential Omp85-related proteins in the chloroplast outer envelope membrane. Plant Physiol 157:147-159.

Irizarry, R.A., Hobbs, B., Collin, F., Beazer-Barclay, Y.D., Antonellis, K.J., Scherf, U., and Speed, T.P. (2003). Exploration, normalization, and summaries of high density oligonucleotide array probe level data. Biostatistics 4:249-264.

Joyard, J., Ferro, M., Masselon, C., Seigneurin-Berny, D., Salvi, D., Garin, J., and Rolland, N. (2009). Chloroplast proteomics and the compartmentation of plastidial isoprenoid biosynthetic pathways. Mol Plant 2:1154-1180.

Kim, C., and Apel, K. (2013). Singlet oxygen-mediated signaling in plants: moving from flu to wild type reveals an increasing complexity. Photosynth Res 116:455-464.

Kim, C., Meskauskiene, R., Apel, K., and Laloi, C. (2008). No single way to understand singlet oxygen signalling in plants. EMBO Rep 9:435-439.

Kim, S., Schlicke, H., Van Ree, K., Karvonen, K., Subramaniam, A., Richter, A., Grimm, B., and Braam, J. (2013). Arabidopsis Chlorophyll Biosynthesis: An Essential Balance between the Methylerythritol Phosphate and Tetrapyrrole Pathways. Plant Cell.

Kindgren, P., Noren, L., Lopez Jde, D., Shaikhali, J., and Strand, A. (2012). Interplay between Heat Shock Protein 90 and HY5 controls PhANG expression in response to the GUN5 plastid signal. Mol Plant 5:901-913.

Kropat, J., Oster, U., Rudiger, W., and Beck, C.F. (2000). Chloroplast signalling in the light induction of nuclear HSP70 genes requires the accumulation of chlorophyll precursors and their accessibility to cytoplasm/nucleus. Plant J 24:523-531.

Laloi, C., Stachowiak, M., Pers-Kamczyc, E., Warzych, E., Murgia, I., and Apel, K. (2007). Cross-talk between singlet oxygen- and hydrogen peroxide-dependent signaling of stress responses in Arabidopsis thaliana. Proc Natl Acad Sci U S A 104:672-677.

Larkin, R.M., Alonso, J.M., Ecker, J.R., and Chory, J. (2003). GUN4, a regulator of chlorophyll synthesis and intracellular signaling. Science 299:902-906.

Leister, D. (2005). Origin, evolution and genetic effects of nuclear insertions of organelle DNA. Trends Genet 21:655-663.

Lermontova, I., and Grimm, B. (2006). Reduced activity of plastid protoporphyrinogen oxidase causes attenuated photodynamic damage during high-light compared to low-light exposure. Plant J 48:499-510.

Livak, K.J., and Schmittgen, T.D. (2001). Analysis of relative gene expression data using real-time quantitative PCR and the 2(-Delta Delta C(T)) Method. Methods 25:402-408.

Martin, W., Rujan, T., Richly, E., Hansen, A., Cornelsen, S., Lins, T., Leister, D., Stoebe, B., Hasegawa, M., and Penny, D. (2002). Evolutionary analysis of Arabidopsis, cyanobacterial, and chloroplast genomes reveals plastid phylogeny and thousands of cyanobacterial genes in the nucleus. Proc Natl Acad Sci U S A 99:12246-12251.

Mauzerall, D., and Granick, S. (1956). The occurrence and determination of delta-amino-levulinic acid and porphobilinogen in urine. J Biol Chem 219:435-446.

McCormac, A.C., and Terry, M.J. (2004). The nuclear genes Lhcb and HEMA1 are differentially sensitive to plastid signals and suggest distinct roles for the GUN1 and GUN5 plastid-signalling pathways during de-etiolation. Plant J 40:672-685.

Meskauskiene, R., Nater, M., Goslings, D., Kessler, F., op den Camp, R., and Apel, K. (2001). FLU: a negative regulator of chlorophyll biosynthesis in Arabidopsis thaliana. Proc Natl Acad Sci U S A 98:12826-12831.

Mochizuki, N., Brusslan, J.A., Larkin, R., Nagatani, A., and Chory, J. (2001). Arabidopsis genomes uncoupled 5 (GUN5) mutant reveals the involvement of Mg-chelatase H subunit in plastid-to-nucleus signal transduction. Proc Natl Acad Sci U S A 98:2053-2058.

Mochizuki, N., Tanaka, R., Grimm, B., Masuda, T., Moulin, M., Smith, A.G., Tanaka, A., and Terry, M.J. (2010). The cell biology of tetrapyrroles: a life and death struggle. Trends Plant Sci 15:488-498.

Mochizuki, N., Tanaka, R., Tanaka, A., Masuda, T., and Nagatani, A. (2008). The steady-state level of Mg-protoporphyrin IX is not a determinant of plastid-to-nucleus signaling in Arabidopsis. Proc Natl Acad Sci U S A 105:15184-15189.

Moore, I., Samalova, M., and Kurup, S. (2006). Transactivated and chemically inducible gene expression in plants. Plant J 45:651-683.

Moulin, M., McCormac, A.C., Terry, M.J., and Smith, A.G. (2008). Tetrapyrrole profiling in Arabidopsis seedlings reveals that retrograde plastid nuclear signaling is not due to Mg-protoporphyrin IX accumulation. Proc Natl Acad Sci U S A 105:15178-15183.

Mullineaux, P., Ball, L., Escobar, C., Karpinska, B., Creissen, G., and Karpinski, S. (2000). Are diverse signalling pathways integrated in the regulation of arabidopsis antioxidant defence gene expression in response to excess excitation energy? Philos Trans R Soc Lond B Biol Sci 355:1531-1540.

Nagai, S., Koide, M., Takahashi, S., Kikuta, A., Aono, M., Sasaki-Sekimoto, Y., Ohta, H., Takamiya, K., and Masuda, T. (2007). Induction of isoforms of tetrapyrrole biosynthetic enzymes, AtHEMA2 and AtFC1, under stress conditions and their physiological functions in Arabidopsis. Plant Physiol 144:1039-1051.

Nott, A., Jung, H.S., Koussevitzky, S., and Chory, J. (2006). Plastid-to-nucleus retrograde signaling. Annu Rev Plant Biol 57:739-759.

Oelmuller, R., and Mohr, H. (1986). Photooxidative destruction of chloroplasts and its consequences for expression of nuclear genes. Planta 167:106-113.

op den Camp, R.G., Przybyla, D., Ochsenbein, C., Laloi, C., Kim, C., Danon, A., Wagner, D., Hideg, E., Gobel, C., Feussner, I., et al. (2003). Rapid induction of distinct stress responses after the release of singlet oxygen in Arabidopsis. Plant Cell 15:2320-2332.

Papenbrock, J., and Grimm, B. (2001). Regulatory network of tetrapyrrole biosynthesis--studies of intracellular signalling involved in metabolic and developmental control of plastids. Planta 213:667-681.

Papenbrock, J., Mock, H.P., Tanaka, R., Kruse, E., and Grimm, B. (2000). Role of magnesium chelatase activity in the early steps of the tetrapyrrole biosynthetic pathway. Plant Physiol 122:1161-1169.

Pesaresi, P., Schneider, A., Kleine, T., and Leister, D. (2007). Interorganellar communication. Curr Opin Plant Biol 10:600-606.

Peter, E., and Grimm, B. (2009). GUN4 is required for posttranslational control of plant tetrapyrrole biosynthesis. Mol Plant 2:1198-1210.

Pfannschmidt, T., Brautigam, K., Wagner, R., Dietzel, L., Schroter, Y., Steiner, S., and Nykytenko, A. (2009). Potential regulation of gene expression in photosynthetic cells by redox and energy state: approaches towards better understanding. Ann Bot 103:599-607.

Pogson, B.J., Woo, N.S., Forster, B., and Small, I.D. (2008). Plastid signalling to the nucleus and beyond. Trends Plant Sci 13:602-609.

Pontier, D., Albrieux, C., Joyard, J., Lagrange, T., and Block, M.A. (2007). Knock-out of the magnesium protoporphyrin IX methyltransferase gene in Arabidopsis. Effects on chloroplast development and on chloroplast-to-nucleus signaling. J Biol Chem 282:2297-2304.

Pontoppidan, B., and Kannangara, C.G. (1994). Purification and partial characterisation of barley glutamyl-tRNA(Glu) reductase, the enzyme that directs glutamate to chlorophyll biosynthesis. Eur J Biochem 225:529-537.

Pulido, P., Spinola, M.C., Kirchsteiger, K., Guinea, M., Pascual, M.B., Sahrawy, M., Sandalio, L.M., Dietz, K.J., Gonzalez, M., and Cejudo, F.J. (2010). Functional analysis of the pathways for 2-Cys peroxiredoxin reduction in Arabidopsis thaliana chloroplasts. J Exp Bot 61:4043-4054.

Ramel, F., Birtic, S., Ginies, C., Soubigou-Taconnat, L., Triantaphylides, C., and Havaux, M. (2012). Carotenoid oxidation products are stress signals that mediate gene responses to singlet oxygen in plants. Proc Natl Acad Sci U S A 109:5535-5540.

Richter, A.S., Peter, E., Rothbart, M., Schlicke, H., Toivola, J., Rintamaki, E., and Grimm, B. (2013). Posttranslational Influence of NADPH-Dependent Thioredoxin Reductase C on Enzymes in Tetrapyrrole Synthesis. Plant Physiol 162:63-73.

Rizhsky, L., Davletova, S., Liang, H., and Mittler, R. (2004). The zinc finger protein Zat12 is required for cytosolic ascorbate peroxidase 1 expression during oxidative stress in Arabidopsis. J Biol Chem 279:11736-11743.

Rodermel, S. (2001). Pathways of plastid-to-nucleus signaling. Trends Plant Sci 6:471-478.

Ruckle, M.E., DeMarco, S.M., and Larkin, R.M. (2007). Plastid signals remodel light signaling networks and are essential for efficient chloroplast biogenesis in Arabidopsis. Plant Cell 19:3944-3960.

Scharfenberg, M., Mittermayr, L., E, V.O.N.R.-L., Schlicke, H., Grimm, B., Leister, D., and Kleine, T. (2013). Functional characterization of the two ferrochelatases in Arabidopsis thaliana. Plant Cell Environ.

Smyth, G.K. (2004). Linear models and empirical bayes methods for assessing differential expression in microarray experiments. Statistical applications in genetics and molecular biology 3:Article3.

Srivastava, A., Lake, V., Nogaj, L.A., Mayer, S.M., Willows, R.D., and Beale, S.I. (2005). The Chlamydomonas reinhardtii gtr gene encoding the tetrapyrrole biosynthetic enzyme glutamyl-trna reductase: structure of the gene and properties of the expressed enzyme. Plant Mol Biol 58:643-658.

Strand, A., Asami, T., Alonso, J., Ecker, J.R., and Chory, J. (2003). Chloroplast to nucleus communication triggered by accumulation of Mg-protoporphyrinIX. Nature 421:79-83.

Susek, R.E., Ausubel, F.M., and Chory, J. (1993). Signal transduction mutants of Arabidopsis uncouple nuclear CAB and RBCS gene expression from chloroplast development. Cell 74:787-799.

Terry, M.J., and Smith, A.G. (2013). A model for tetrapyrrole synthesis as the primary mechanism for plastid-to-nucleus signaling during chloroplast biogenesis. Frontiers in plant science 4:14.

Voigt, C., Oster, U., Bornke, F., Jahns, P., Dietz, K.J., Leister, D., and Kleine, T. (2010). In-depth analysis of the distinctive effects of norflurazon implies that tetrapyrrole biosynthesis, organellar gene expression and ABA cooperate in the GUN-type of plastid signalling. Physiol Plant 138:503-519.

von Gromoff, E.D., Alawady, A., Meinecke, L., Grimm, B., and Beck, C.F. (2008). Heme, a plastid-derived regulator of nuclear gene expression in Chlamydomonas. Plant Cell 20:552-567.

Wielopolska, A., Townley, H., Moore, I., Waterhouse, P., and Helliwell, C. (2005). A high-throughput inducible RNAi vector for plants. Plant Biotechnol J 3:583-590.

Woodson, J.D., and Chory, J. (2012). Organelle signaling: how stressed chloroplasts communicate with the nucleus. Curr Biol 22:R690-692.

Woodson, J.D., Perez-Ruiz, J.M., and Chory, J. (2011). Heme synthesis by plastid ferrochelatase I regulates nuclear gene expression in plants. Curr Biol 21:897-903.

Xiao, Y., Savchenko, T., Baidoo, E.E., Chehab, W.E., Hayden, D.M., Tolstikov, V., Corwin, J.A., Kliebenstein, D.J., Keasling, J.D., and Dehesh, K. (2012). Retrograde signaling by the plastidial metabolite MEcPP regulates expression of nuclear stress-response genes. Cell 149:1525-1535.

Fig. 1

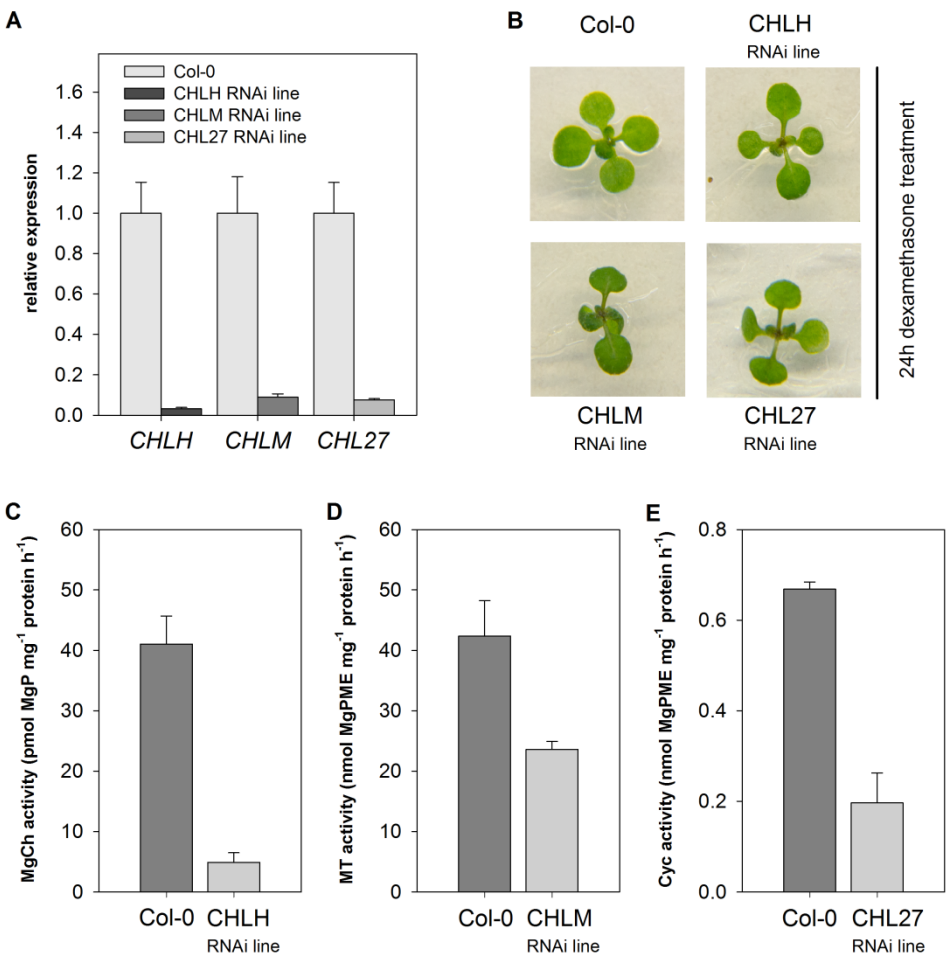

Figure 1. Genetic and biochemical analysis of transgenic lines after 24 h gene silencing of *CHLH*, *CHLM* and *CHL27*, respectively.

(A) Transcript analysis of 10-day-old seedlings of the CHLH, CHLM and CHL27 RNAi lines growing on MS medium in continuous light 24 h after induced gene silencing. Transcript levels were calculated as relative expression ($2^{-\Delta\Delta CT}$) according to (Livak and Schmittgen, 2001) in comparison to dexamethasone-treated wild-type plants as control and *Actin2* as a reference gene. The *CHLH*, *CHLM* and *CHL27* transcript contents were decreased in the corresponding RNAi lines to less than 10% of the wild type content. Data are given as means and SD of three biological replicates. (B) Phenotypes of 14-day-old *Arabidopsis* wild-type and RNAi lines. Seedlings grew in continuous light of 100 µmol photon m^{-2} s^{-1} treated for 24 h with dexamethasone. (C-E) Enzyme activity assays with crude *Arabidopsis* chloroplast extracts 24 h after induction of RNAi silencing for (C) Mg chelatase (MgCh), (D) MgP methyltransferase (MT) and (E) MgPME cyclase (Cyc). Data are given as means and SD of three biological replicates. All experiments were repeated at least two times.

Fig. 2

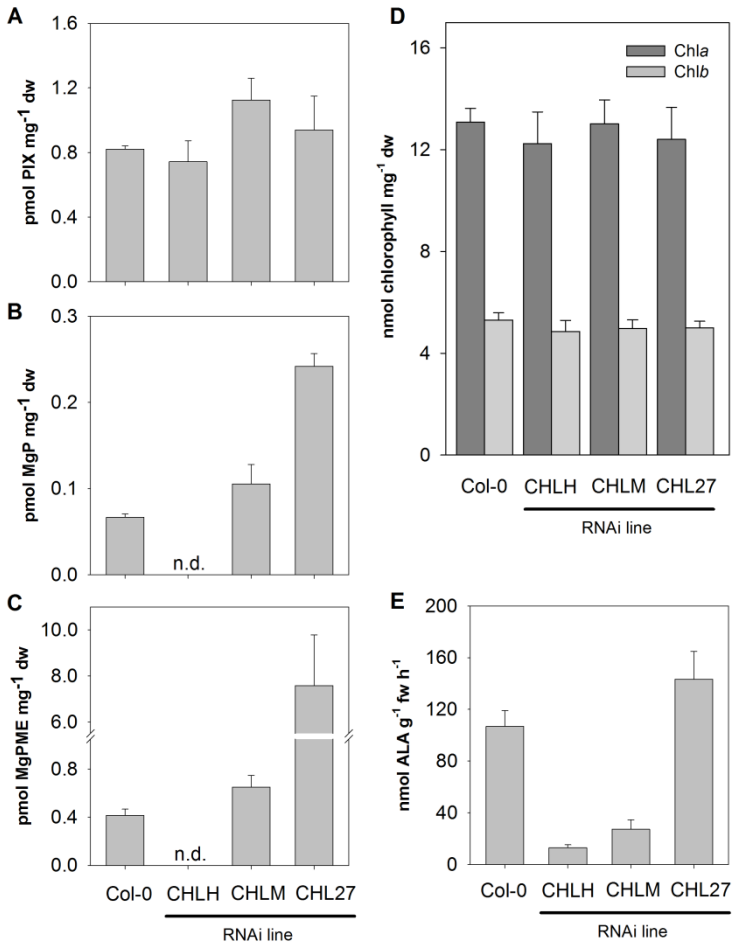

Figure 2. Chlorophyll content and steady state levels of tetrapyrrole biosynthesis intermediates 24 h after *CHLH*, *CHLM* and *CHL27* gene silencing.

(A-C) Steady state levels of porphyrins 24 h after treatment with dexamethasone and induced RNAi gene silencing. A. protoporphyrin IX (PIX), B. magnesium protoporphyrin (MgP), C. MgP monomethylester (MgPME). (D) The chlorophyll content of seedlings of the three RNAi lines and wild type determined 24 h after induced gene silencing. (E) Analysis of the ALA synthesizing capacity in transgenic lines in comparison to wild type after 24 h of induced *CHLH*, *CHLM* and *CHL27* gene silencing. Plants were grown on soil for 14 days under 100 µmol photon m^{-2} s^{-1} light intensity.

Fig. 3

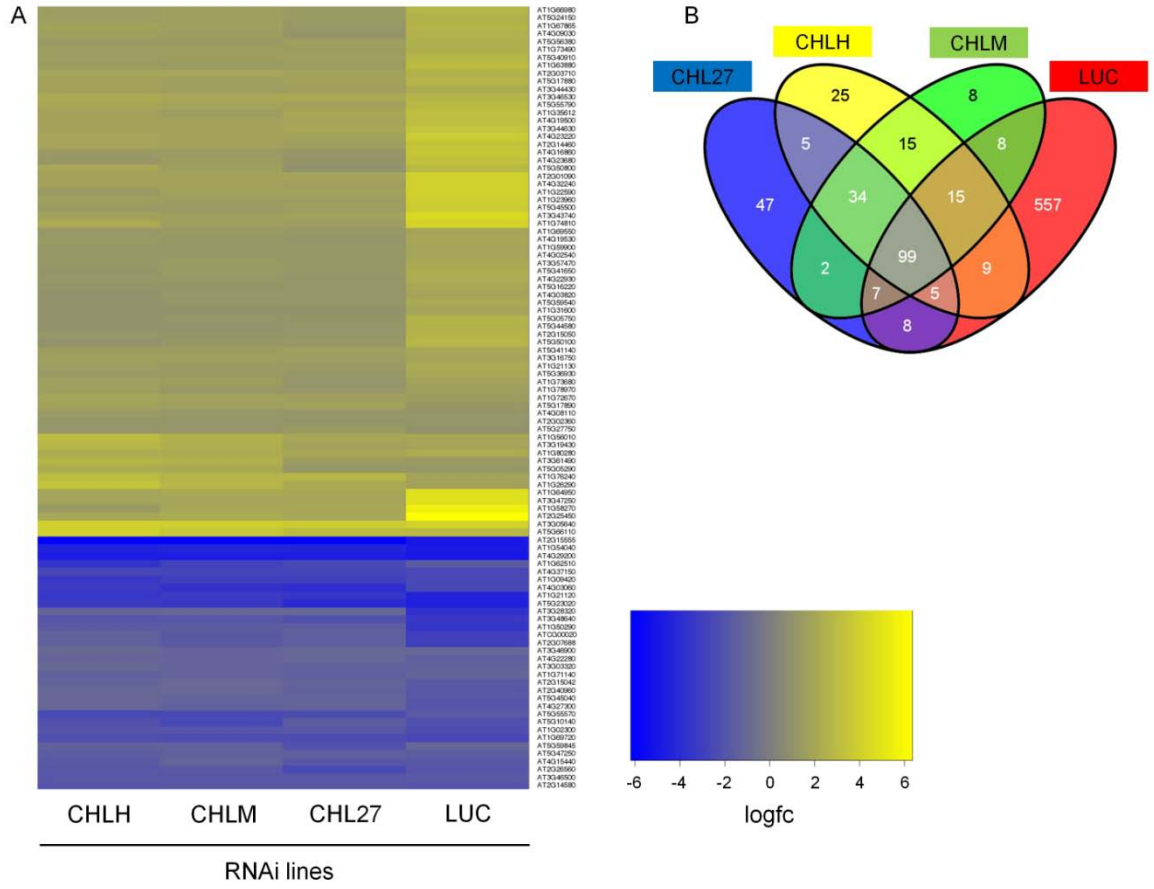

Figure 3. Comparative microarray analysis of CHLH, CHLM, CHL27 and LUC RNAi lines 24 h after RNAi induction.

(A) Heat map analysis of commonly deregulated genes 24 h after induction of RNAi in the four RNAi lines. The LUC RNAi line contains a part of the firefly luciferase gene sequence which did not interfere with *Arabidopsis thaliana* transcripts after activation of the RNAi machinery. Genes showing a twofold increase or decrease of the fold change (FC) compared to wild type and a *P*-value of less than 0.05 in all four RNAi lines were depicted. Almost all these genes are uniformly deregulated. (B) The Venn diagram shows the central cluster of 99 commonly deregulated genes 24 h after dexamethasone activation of the RNAi mechanism. The intersections represent the number of mutually deregulated genes in the corresponding RNAi lines. The Supplemental Table 3 contains the lists of genes representing the intersections.

Fig. 4

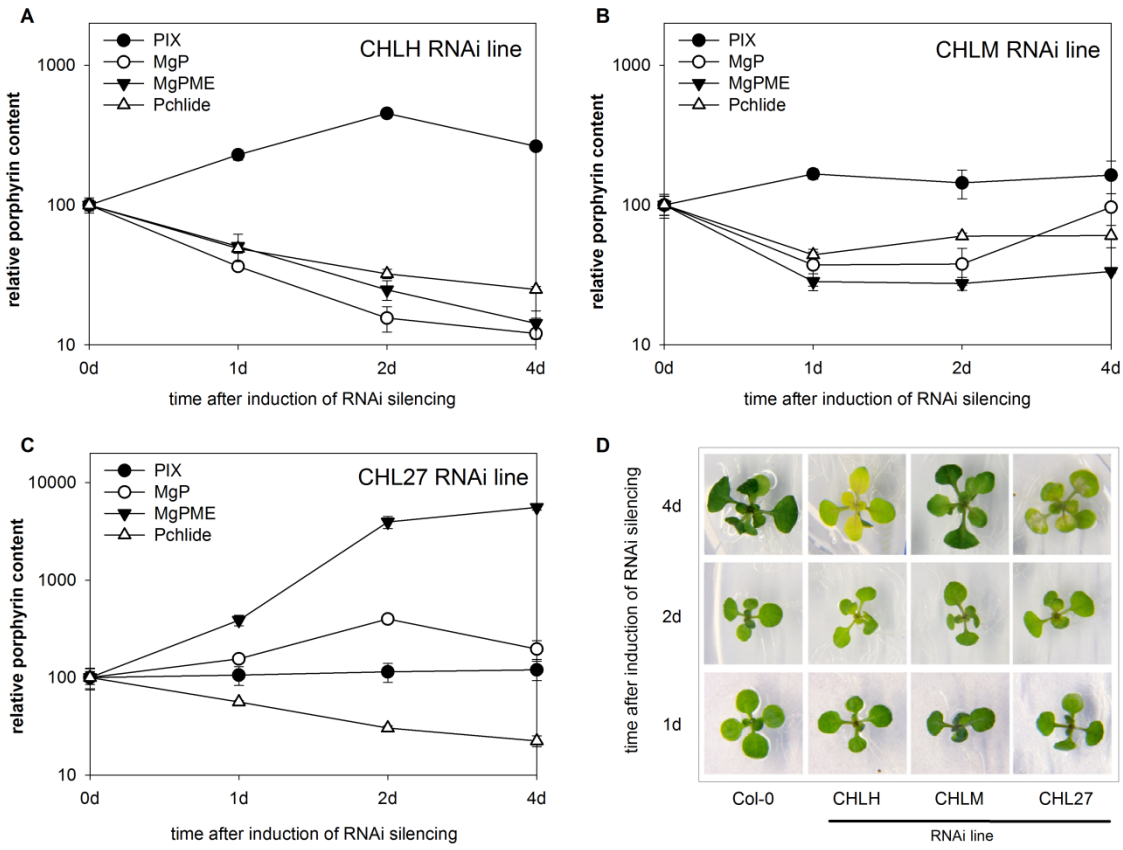

Figure 4. Kinetics on steady state levels of PIX and Mg porphyrins within a 4-day-silencing of genes encoding proteins of chlorophyll biosynthesis.

(A-C) Time course of porphyrin steady state levels 1, 2 and 4 days after induced RNAi gene silencing of *CHLH*, *CHLM* and *CHL27* compared to the time point t_0. PIX, protoporphyrin, MgP, magnesium protoporphyrin, MgPME, MgP monomethylester, and Pchlide, protochlorophyllide were analyzed. (D) Phenotypes of *Arabidopsis* wild-type and RNAi lines seedlings growing in continuous light of 100 µmol photon m^{-2} s^{-1} after a long-term dexamethasone-induced *CHLH*, *CHLM* or *CHL 27* gene silencing.

Fig. 5

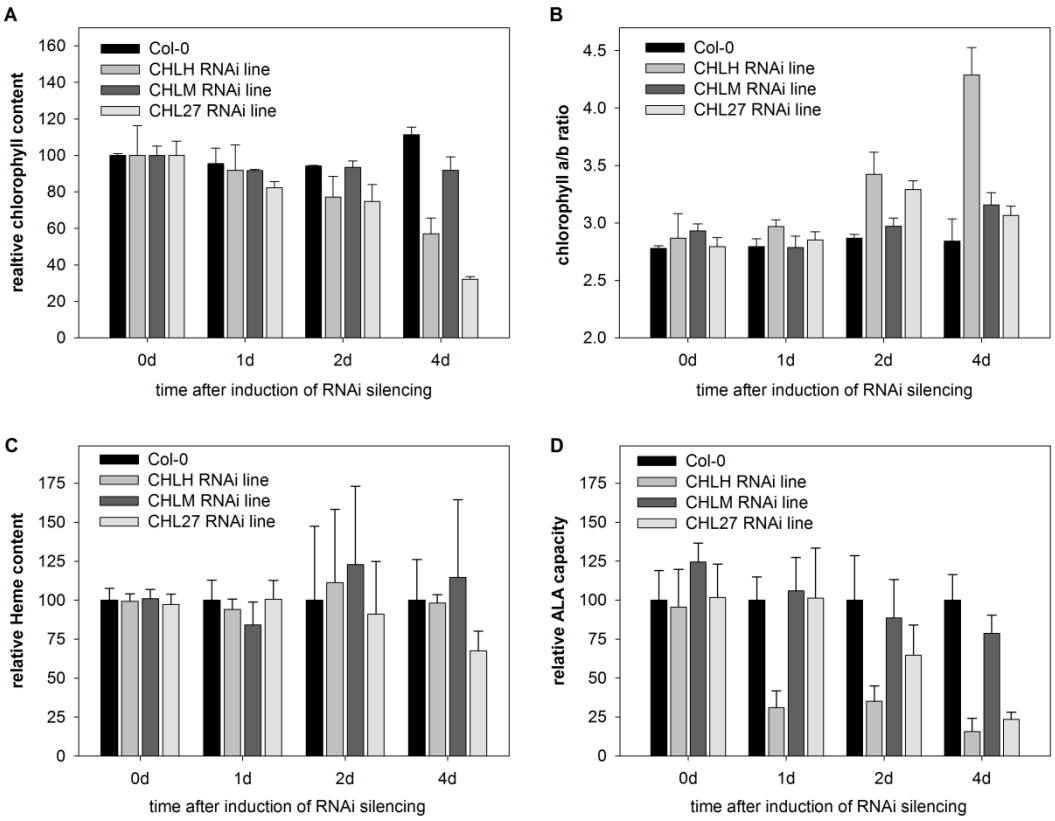

Figure 5. Analysis of chlorophyll and heme content as well as ALA capacity in wild type and transgenic RNAi lines in the course of 4-day deactivation of early enzymatic steps in the Mg branch of tetrapyrrole biosynthesis.

(A) Relative chlorophyll content compared to time point t_0 for each line. The wild type chlorophyll content at time point t_0 is 12.2 nmol mg^{-1} dw. (B) The chlorophyll *a* /chlorophyll *b* ratio in wild type and the three RNAi lines. (C) Relative heme content in of transgenic lines compared to wild type for each time point. The wild type has a heme content of 1.2 pmol mg^{-1} dw at t_0. The heme content is not significantly altered in the RNAi lines within the 4 days of gene inactivation. (D) ALA synthesizing capacity of the three RNAi lines compared to wild type for each time point. The t_0 value of wild type corresponds to 0.36 nmol ALA mg^{-1} fw h^{-1}.

Fig. 6

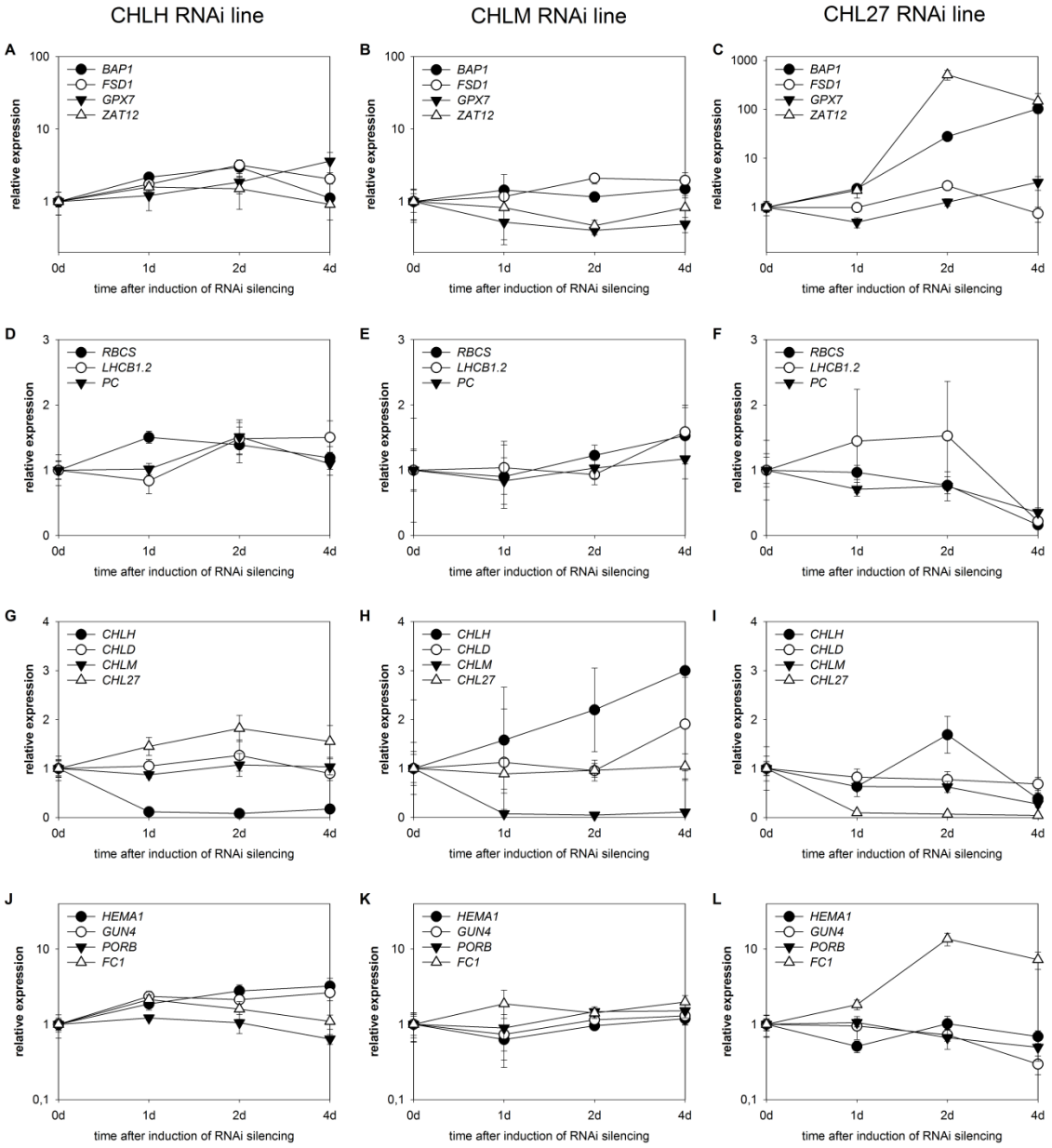

Figure 6. Analysis of the transcript levels of nuclear genes in the CHLH, CHLM and CHL27 RNAi lines during a time course of 4-day-induction of RNAi.

(A-C) Transcript analysis of ROS marker genes. *BAP1* a $^1O_2$-responsive gene and *ZAT12* a H_2O_2 responsive gene encoding bonzai1-associated protein 1 and zinc finger protein, respectively. *GPX7* and *FSD1* encode the plastid-localized glutathione peroxidase 7 and Fe-superoxide dismutase, respectively. (D-F) Transcript analysis of the representatives of PhANGs, *RBCS*, *LHCB1.2* and *PC* encoding ribulose 1,5-bisphosphate carboxylase small subunit, LHCB of photosystem II and plastocyanin, respectively.(G-I) Analysis of mRNA amounts of genes encoding enzymes of the Mg branch of tetrapyrrole biosynthesis. *CHLH*

and *CHLD* encode the CHLH and CHLD subunit of Mg chelatase. *CHLM* and *CHL27* encode MgP methyltransferase and the CHL27 subunit of MgPME cyclase, respectively. (J-L) Analysis of mRNA amounts of genes encoding target proteins of tetrapyrrole biosynthesis. *HEMA1*, *GUN4*, *PORB* and *FC1* encode the glutamyl-tRNA reductase 1, GUN4, a positive regulator of the Mg chelatase reaction, protochlorophyllide oxidoreductase B and ferrochelatase 1, respectively. Transcript levels were calculated as relative expression ($2^{-\Delta\Delta CT}$) according to (Livak and Schmittgen, 2001) in comparison to t_0 and *Actin2* as a reference gene. Data are given as means and SD of three biological replicates summarized in the Supplemental Table 6. Plants were grown on MS for 14 days under continuous light (100 µmol photon m^{-2} s^{-1}). Data shown as logarithmic scale (Figure A-C and J-L) or linear scale (Figure D-I).